Nuclear signaling by Rac and Rho GTPases is required in the establishment of epithelial planar polarity in the *Drosophila* eye

Manolis Fanto*†, Ursula Weber†, David I. Strutt‡ and Marek Mlodzik†

Background: The small GTPases Rac and Rho act as cellular switches in many important biological processes. In the fruit fly *Drosophila*, RhoA participates in the establishment of planar polarity, a process mediated by the receptor Frizzled (Fz). Thus far, analysis of Rac in this process has not been possible because of the absence of mutant *Rac* alleles. Here, we have investigated the role of Rac and Rho in establishing the polarity of ommatidia in the *Drosophila* eye.

Results: By expressing a dominant negative or a constitutively activated form of Rac1, we interfered specifically with Rac signaling and disrupted ommatidial polarity. The resulting defects were similar to the loss/gain-of-function phenotypes typical of tissue-polarity genes. Through genetic interaction and rescue experiments involving a polarity-specific, loss-of-function *dishevelled* (*dsh*) allele, we found that Rac1 acts downstream of Dsh in the Fz signaling pathway, but upstream of, or in parallel to, RhoA. Rac signaled to the nucleus through the Jun N-terminal kinase (JNK) cascade in this process. By generating point mutations in the effector loop of RhoA, we found that RhoA also signals to the nucleus during the establishment of ommatidial polarity. Nevertheless, Rac and RhoA activated transcription of distinct target genes.

Conclusions: Rac is specifically required downstream of Dsh in the Fz pathway. It functions upstream or in parallel to RhoA and both signal to the nucleus, through distinct effectors, to establish planar polarity in the *Drosophila* eye.

Address: EMBL, Developmental Biology Programme, Meyerhofstraße 1, D-69117 Heidelberg, Germany.

Present addresses: *†ICRF, Lincoln's Inn Fields, London WC2A 3PX, UK. †Mount Sinai School of Medicine, Department of Cell Biology and Anatomy, One Gustave L. Levy Place, New York, New York 10029, USA. ‡Developmental Genetics Programme, University of Sheffield, Firth Court, Western Bank, Sheffield S10 2TN, UK.

Correspondence: Marek Mlodzik
E-mail: mlodzik@embl-heidelberg.de

Received: **13 December 1999**
Revised: **31 May 2000**
Accepted: **28 June 2000**

Published: **1 August 2000**

Current Biology 2000, 10:979–988

0960-9822/00/$ – see front matter

Background

In *Drosophila*, the Rho subfamily of small GTPases consists of at least five proteins, RhoA (or Rho1), RhoL, Rac1, Rac2 and Cdc42 [1–3]. Expression of constitutively activated and dominant-negative isoforms has suggested important roles for Rac1 and Cdc42 in axonal outgrowth, muscle development and embryonic dorsal closure [1,2,4]. Recently, the establishment of epithelial planar polarity (EPP) in *Drosophila* has emerged as a good model system to study the role(s) of Rho family GTPases, as both RhoA and Rac1 have been implicated in the process [5,6].

In the *Drosophila* eye, EPP is manifest in the mirror-symmetric arrangement of ommatidia relative to the dorsoventral midline, the equator. The photoreceptors within each ommatidium are arranged in an asymmetric trapezoidal shape, with the R7 photoreceptor pointing towards the equator and R3 towards the polar side. In the wild type, ommatidia of opposite chirality lie on either side of the equator, which represents an axis of mirror symmetry (all ommatidia adopt the same chiral form in a given half of the eye; for reviews, see [7–9]).

The formation of this cellular pattern begins in the early third instar imaginal disc, when the morphogenetic furrow (MF) passes across the eye disc from posterior to anterior [10–12]. Cells within the epithelium are unpatterned until the furrow passes through. In and behind the MF, cells begin to organize themselves into ommatidial preclusters. When these initially emerge from the furrow, they are arranged symmetrically in the anteroposterior (AP) axis. Subsequently, they rotate first by 45° towards the equator (in opposite directions in either half of the eye disc). They maintain this angle for a few rows before rotating by a further 45°, and are thus 90° to the original AP axis, establishing the equator as an axis of mirror symmetry. At the end of rotation, the ommatidia lose their symmetry, with the R3 precursor displacing R4, establishing chirality [7–9].

The tissue-polarity genes of *Drosophila* are required for correct EPP establishment in all adult epidermal structures [13,14]. In the eye, mutations in tissue-polarity genes, such as *frizzled* (*fz*) and *dishevelled* (*dsh*), result in loss of mirror-image symmetry: ommatidial preclusters rotate randomly and acquire random chirality. In some cases, the R3/R4 cells do not realign themselves, giving rise to non-chiral, symmetrical ommatidia [15,16]. The *fz* gene encodes a seven-pass transmembrane protein with some characteristics of G-protein-coupled receptors, and is

required for reception and transmission of an EPP signal [17,18]. Fz proteins have been identified as the receptors for the Wnt family of growth factors [19–24]. The canonical Wnt signaling cascade is, however, not involved in EPP generation [25,26]. Until recently, little was known about the nature of the signaling pathway(s) involved in establishing planar polarity, except that Dsh acts downstream of Fz [6,27]. Other genes required in the process, such as *nemo* and *roulette* (*rlt*) specifically affect ommatidial rotation, but not the establishment of chirality and direction of rotation [28]. The *nemo* mutant fails to complete rotation of the clusters and remains arrested after the first 45°; in the *rlt* mutant, ommatidia rotate to random degrees. Thus, *nemo* and *rlt* are considered effectors of the rotation process, acting at later stages than the primary polarity genes of the Fz pathway.

Members of the Rho subfamily have also been implicated in the establishment of planar polarity. In the wing, expression of $Cdc42^{N17}$, a dominant-negative protein form of Cdc42, affects cell shape in discs and actin polymerization during wing hair formation. Rac^{N17} in contrast disrupts adherens junctions and the polarity of wing hairs [5,29]. In *Drosophila*, *RhoA* mutants display EPP phenotypes in eyes and wings [6]. Moreover, the gain-of-function phenotypes resulting from expression of *fz* or *dsh* transgenes under the control of promoter/enhancer elements of the *sevenless* gene (*sev–Fz* and *sev–Dsh*, respectively) are dominantly suppressed by a reduction in the gene dosage of *RhoA*. This suggests that *RhoA* is part of the 'primary' planar-polarity genes and that it acts downstream of Fz and Dsh. Finally, it has been shown that *sev–Dsh* is dominantly suppressed by deficiencies that remove *Rac1* and *Rac2*, whereas removal of *Dcdc42* does not have an effect on *sev–Dsh* [26]. Here, we have investigated the role of Rho subfamily members in the generation of planar polarity in the eye. Rac and RhoA were both found to signal to the nucleus during this process and, like Fz and Dsh, they also activated transcription of *Delta*.

Results

Loss-of-function and gain-of-function Rac1 isoforms interfere with ommatidial polarization

The genetic suppression of *sev–Dsh* by deficiencies that remove *Drac1* and *Drac2* suggests that *Rac* genes might be involved in EPP signaling [26]. In contrast, *DCdc42* mutants do not interact with *sev–Fz* or *sev–Dsh* [6,26]. Similarly, a dominant-negative *Drosophila* Rac1 isoform, Rac^{N17}, affects polarity of the wing hairs, whereas the equivalent Cdc42 mutations affect actin polymerization but not wing-hair polarity [29]. A simple loss-of-function analysis of the *Rac* genes is hampered by the fact that specific mutant alleles exist for neither *DRac1* nor *DRac2*. This is possibly due to their high degree of homology (> 95% identity) and associated redundancy. They are both expressed uniformly throughout the imaginal discs [3].

To determine whether Rac is a component of EPP signaling in the eye, we expressed Rac^{N17} transiently in the developing eye imaginal disc in R3/R4, the photoreceptor precursor pair that is important for polarity establishment, under the control of *sev–GAL4* (see Materials and methods; henceforth referred to as *sev>*Rac^{N17}). Interestingly, *sev>*Rac^{N17} eyes had planar-polarity defects (Figure 1a,b), and this phenotype was further enhanced by *Df(3L)emc5*, which removes the *Rac1* gene (Figure 2b,d–f), indicating that Rac activity is specifically involved in EPP establishment. Although it was mostly ommatidial rotation that was randomized in *sev>*Rac^{N17} eyes, and ommatidia that adopted incorrect chiral forms were rare, the enhancement of the *sev>*Rac^{N17} phenotype by the *Rac1* deficiency (as well as by *RhoA* loss-of-function alleles, see below) increased the number of symmetrical, achiral ommatidia (Figure 2f; see also Discussion). This phenotype resembled that of *fz* and *dsh* mutants [15,16], rather than that of *nemo* and *rlt* [28], suggesting a function for Rac in the Fz pathway.

To test whether a gain-of-function mutation in Rac1 could also generate a polarity phenotype, we expressed a constitutively active form of Drac1 under the control of *sev* promoter/enhancer sequences (*sev–*Rac^{V12}; see Materials and methods). The *sev–*Rac^{V12} transgene resulted in the misorientation of many ommatidia (Figure 1c), with some also displaying defects in chirality, such as the adoption of the wrong chiral form or remaining symmetrical. Interestingly, the symmetrical clusters were always of the R3/R3 type (Figure 1c), which is reminiscent of the *sev–Fz* gain-of-function phenotype. The *sev–*Rac^{V12} transgene also interferes with photoreceptor recruitment or differentiation. Expression of wild-type Rac1 (under the control of *sev* control elements) did not produce any defects, indicating that the phenotypes described are caused by dominant-active Rac1 and constitutively active $Rac1^{V12}$, and not due to a non-specific consequence of overexpressing any form of the GTPase.

To establish whether the polarity defects observed with *sev>*Rac^{N17} and *sev–*Rac^{V12} arise early in development and are thus primary, direct defects, we used the *seven-up* (*svp*) enhancer detector line, svp^{07482}, with nuclear β-galactosidase expression early in R3/R4 precursors and later (at lower levels) also in R1/R6. This expression pattern reveals the ordered polarity of ommatidial preclusters from its earliest appearance ([30,31] and Figure 1d). In *sev>*Rac^{N17} and *sev–*Rac^{V12} eye discs, ommatidial polarity was affected early in development (Figure 1e,f): the R3/R4 pairs were often incorrectly oriented with respect to their neighbors and position in the eye disc, either having not started to rotate or having rotated in the opposite direction. This suggested that the polarity phenotype caused by *sev>*Rac^{N17} and *sev–*Rac^{V12} is a primary defect. Taken together, these experiments indicate a requirement for Rac1 in EPP signaling.

Figure 1

Dominant-negative and activated Rac1 isoforms cause planar-polarity defects in the eye. In all figures, anterior is to the left and dorsal is uppermost. **(a–c)** Tangential sections through the equatorial region of adult eyes (upper panels) and schematic representation of ommatidial polarity (lower panels) of (a) wild-type, (b) *sev>Rac^{N17}* and (c) *sev–Rac^{V12}* flies. Correctly oriented ommatidia are indicated by black arrows with a flag (indicating chirality), misrotated ommatidia by red arrows with a flag, and symmetric, achiral ommatidia of the R3/R3 type by green arrows; ommatidia with an incorrect complement of photoreceptors are shown as black circles. The same key is used for all schematic representations in the subsequent figures. **(d–f)** Nuclear β-galactosidase expression from the *svp* enhancer detector line, *svp^{07482}*, in third instar larval eye imaginal discs of (d) wild-type, (e) *sev>Rac^{N17}* and (f) *sev–Rac^{V12}* flies. Expression of *svp–lacZ* is detected early in R3/R4 precursors and later (at lower levels) also in R1/R6. Parts of the dorsal half of the imaginal discs are shown. Upper panels show overlay of β-galactosidase (red) and Elav (green; marks all photoreceptors); lower panels show the red channel (*svp–lacZ*) only. The white and yellow arrows (inserted between the R3/R4 precursors) mark examples of clusters with correct or abnormal orientation, respectively. Note that wild-type clusters first rotate through 30°, then 45°, at which stage the clusters pause. The precursor cells of R3/R4 are numbered in examples.

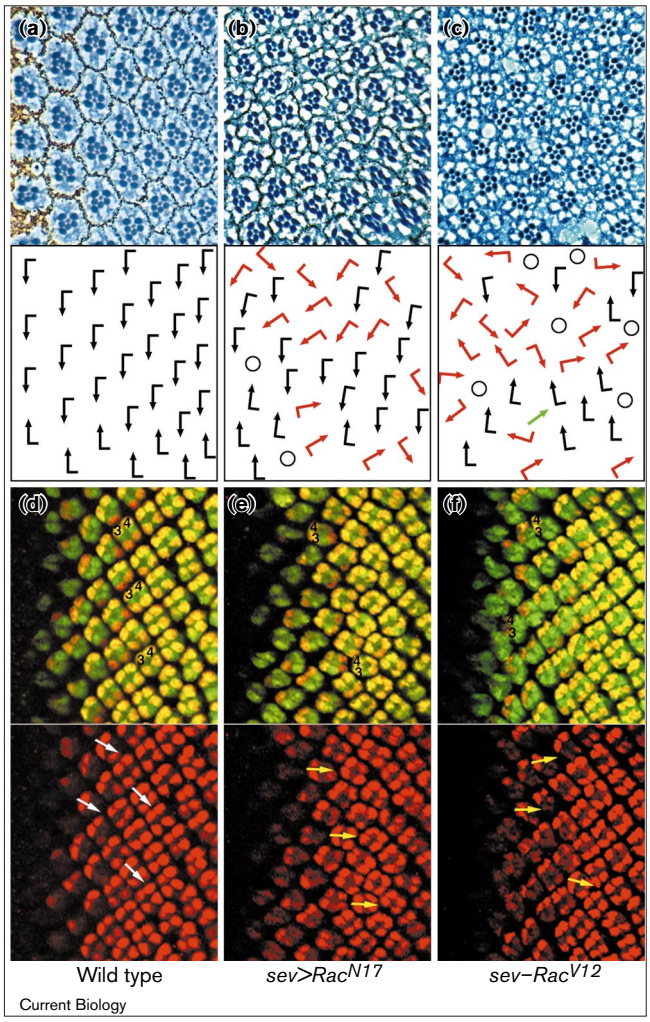

Dsh lies upstream of Rac1 in planar-polarity signaling

Dsh acts cell autonomously, downstream of Fz in the EPP signaling cascade. Genetic experiments have placed RhoA downstream of Dsh [6], and similarly *sev–Dsh* is dominantly suppressed by deficiencies that remove *Rac1* (*Df(3L)emc5*) and *Rac2* (*Df(3L)pblx1*) [26]. This suggests that the *Drosophila* Rac proteins might also act downstream of Dsh.

To further address this issue, we determined whether Rac1 was able to rescue a hypomorphic allele of *dsh*, *dsh^{1}*. The eye-polarity phenotype of *dsh^{1}* can be rescued by *sev*-driven expression of Dsh itself, by a weakly expressed constitutively activated *RhoA* or by any other component of the polarity pathway acting downstream of Dsh, that is, Hemipterous (Hep), Basket (Bsk) and Jun. In contrast, molecules upstream of Dsh, such as Fz, are not able to do so [26]. We tested whether *dsh^{1}* could be rescued by overexpressing wild-type Rac1 (*sev–Rac*), which does not display a dominant phenotype. The presence of *sev–Rac* significantly rescued the *dsh^{1}* eye phenotype, increasing the percentage of correctly polarized ommatidia (Figure 3). This result, taken together with the finding that whereas deficiencies removing the *Rac* genes suppress *sev-Dsh* [26], *sev-Rac^{V12}* is unaffected by removing one copy of *dsh* (Table 1), supports the hypothesis that Rac functions downstream of *dsh*.

RhoA acts downstream or in parallel to Rac1

We further determined whether Rac and RhoA act in a hierarchy in the EPP signaling context. To investigate their relationship to one another in this process, we analyzed their genetic interactions and found that *RhoA* dominantly interacts with both *sev>Rac^{N17}* and *sev–Rac^{V12}*. In particular, reducing the gene dosage of *RhoA* significantly enhanced *sev>Rac^{N17}* (Figure 2c,g), and complementarily suppressed *sev–Rac^{V12}* (Figure 4a,b). The significant increase of the number of achiral ommatidia in *sev>Rac^{N17}*; *RhoA^{-}*/+ flies suggests that the two GTPases co-operate in this context. Moreover, overexpression of wild-type RhoA (*sev–RhoA*) rescued the *sev>Rac^{N17}* phenotype (Figure 2d,h), suggesting that RhoA acts downstream of Rac in this process. We did not see the opposite interactions (that is, a modification of a *RhoA* gain-of-function phenotype by reducing the dosage of *Rac* using deficiencies covering *Rac1* and *Rac2*). This analysis was, however, limited because of the absence of clean loss-of-function alleles of *Rac1* or *Rac2*. Nevertheless, these data are in agreement with the hypothesis that RhoA functions downstream or in parallel to Rac1.

Mutations in the JNK pathway suppress the *sev-Rac^{V12}* phenotype

Mutations in the JNK MAP kinase module can suppress the gain-of-function *sev–Fz* and *sev–Dsh* phenotypes [6,26,32], suggesting that JNK signaling is involved in transmitting Fz signals. In mammalian cell culture assays, Rac (and Cdc42) can activate JNK [33,34]. To test whether

Figure 2

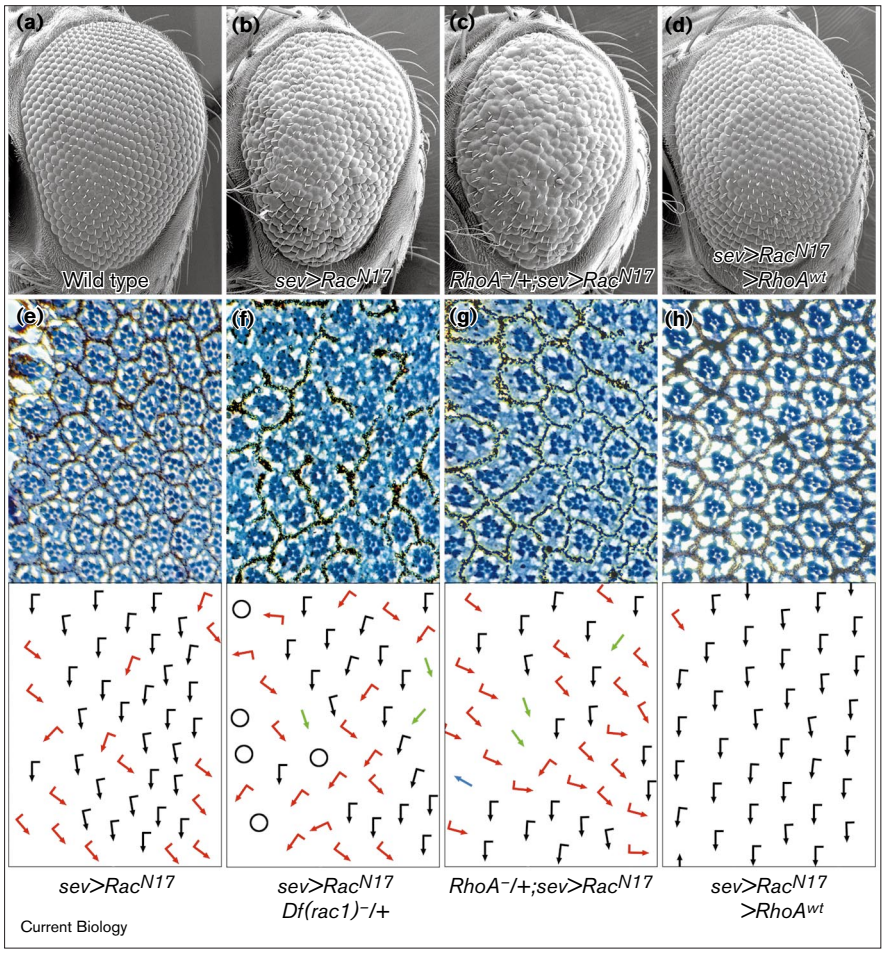

The effects of *sev>Rac^{N17}* are enhanced by *Rac* deficiencies and *RhoA* mutations. **(a–d)** Scanning electron micrographs of eyes of (a) wild-type, (b) *sev>Rac^{N17}*, (c) *sev>Rac^{N17}/+; RhoA^{P2}/+* (indicated as *RhoA^{-}/+; sev>Rac^{N17}* in the figure) and (d) *sev>Rac^{N17}/>Rho^{wt}* flies. **(e–h)** Tangential sections through the dorsal half of the eye (upper panels) and their schematic representation (lower panels) from (e) *sev>Rac^{N17}/+*, (f) *sev>Rac^{N17}/+; Df(3L)emc5 (Rac1^{-})/+*, (g) *sev>Rac^{N17}/+; RhoA^{P2}/+* and (h) *sev>Rac^{N17}/>Rho^{wt}* flies. Arrows are drawn as in Figure 1; symmetrical R3/R3 or R4/R4 type ommatidia are indicated by green and blue arrows, respectively. Quantification of the interactions was derived from 4–6 eyes ($n = 450–700$); the percentage of correctly polarized ommatidia (± SD) was: 65.1 ± 2.0 for *sev>Rac^{N17}/+*, 42.6 ± 2.1 for *sev>Rac^{N17}/+; Df(3L)emc5 (Rac1^{-})/+*, 49.0 ± 3.1 for *sev>Rac^{N17}/+; RhoA^{P2}/+*, and 92.1 ± 3.4 for *sev>Rac^{N17}/>Rho^{wt}*. All interactions were highly significant ($p < 0.001$ in the Student's *t*-test). The number of achiral ommatidia was quantified in three eyes of each genotype (corresponding to 320–370 ommatidia in total): we found 0 in *sev>Rac^{N17}/+*, 14 in *sev>Rac^{N17}/+; Df(3L)emc5 (Rac1^{-})/+* and 12 in *sev>Rac^{N17}/+; RhoA^{P2}/+*.

Rac is upstream of JNK signaling in polarity generation, we analyzed the sensitivity of *sev–Rac^{V12}* to a reduction in gene dosage of components of this cascade. All *basket* (*bsk/JNK*), *hemipterous* (*hep/JNKK*), and *D-jun* (a target of JNK) alleles tested strongly suppressed *sev–Rac^{V12}* (Figure 4), suggesting that they are required downstream of Rac in this process (see Table 1 for quantification).

In contrast, upstream components, such as *fz* and *dsh*, did not display an interaction. This was also the case for components of Wingless (Wg) signaling, confirming that the Wg and EPP pathways are distinct. Moreover, reducing the dosage of MAP kinase signaling components of the Ras or extracellular signal-regulated kinase (ERK) type (for example, mutations in *Ras1*, *rl*, *raf*, and *pnt*; Table 1) did not affect *sev–Rac^{V12}*, suggesting that the JNK cascade is specifically involved downstream of Rac.

We also tested other genes involved in the establishment of ommatidial polarity. Whereas *roulette* [28] and *strabismus* [35] suppressed *sev–Rac^{V12}*, *nemo* [28] and *prickle-spiny legs* [36] did not display any significant interaction (Table 1). The role of these genes and their relationship to Fz signaling is not clear, however (reviewed in [8,9]).

Constitutively activated RhoA leads to polarity defects and loss of photoreceptors

Clones of strong hypomorphic loss of function *RhoA* alleles display a tissue polarity phenotype similar to that of *fz* and *dsh*. RhoA is also required, however, for general cell survival as clones of null alleles cannot be recovered in imaginal disc tissues [6]. To investigate the effect of activated *RhoA*, and to compare its phenotype with that of the *Rac1* gain-of-function mutation, we generated flies expressing RhoA^{V14} under the control of *sev* promoter and enhancer elements (*sev–Rho^{V14}*), and analyzed its effects in imaginal discs and adult eyes. Weak *sev–Rho^{V14}* expression led to photoreceptor loss but not significant polarity defects (Figure 5b). When the transgene was expressed at higher levels (for example, in flies homozygous for the insertion; Figure 5c), polarity defects became apparent. Analysis in imaginal discs using the *svp* enhancer trap line revealed

Figure 3

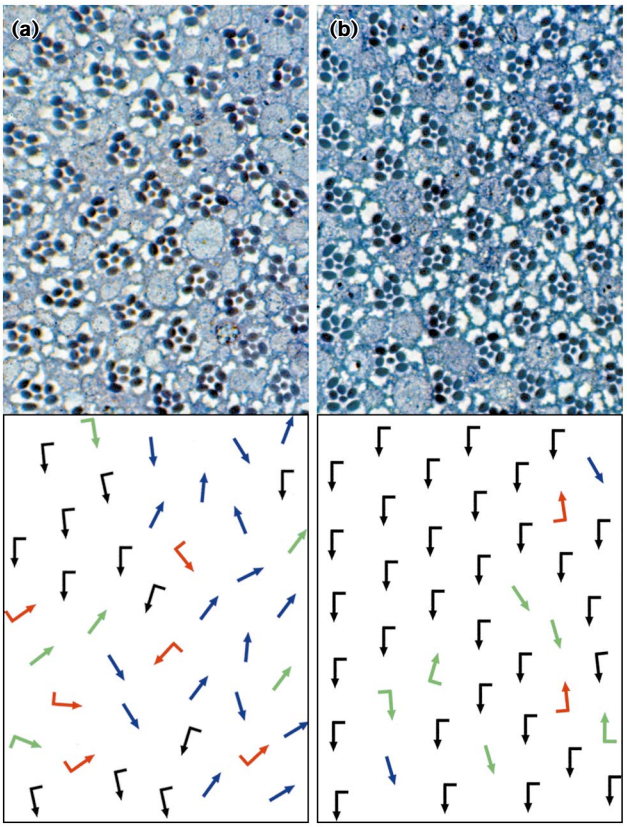

Overexpression of Rac partially rescues a planar-polarity-specific *dsh* allele. Tangential sections and schematic drawings of **(a)** *dsh*^{1}*/Y* and **(b)** *dsh*^{1}*/Y*; *sev–Rac*^{WT}*/+* eyes. Arrows are as in Figures 1 and 2. Green arrows with a flag represent ommatidia that have adopted the wrong (ventral) chirality. Quantification of the interactions ($n = 452–844$ from 4–8 eyes) demonstrated a highly significant rescue ($p < 0.001$ in the Student's *t*-test): 44.5 ± 5.2 for *dsh*^{1}*/Y* and 68.8 ± 4.5 for *dsh*^{1}*/Y*; *sev–Rac/+*.

Table 1

Quantification of the genetic interactions with *sev–Rac*^{V12}.

Genotype *sev–Rac*^{V12}	Ommatidia with abnormal polarity (% ± SD)
w^{1118} (+/+, control)	30.0 ± 2.7
fz^{1}*/+*	25.9 ± 2.8
dsh^{V26}*/+*	35.3 ± 2.1
RhoA^{P2}*/+*	17.7 ± 3.5*
RhoA72R/+	14.1 ± 5.4*
Cdc42^{3}*/+*	30.1 ± 2.0
Df(3L)emc5 (Rac1^{-}*)/+*	13.4 ± 1.7*
hep^{1}*/+*	11.0 ± 1.7*
hep^{r75}*/+*	12.3 ± 3.4*
bsk^{1}*/+*	12.7 ± 4.3*
bsk^{2}*/+*	16.6 ± 4.3*
Djun^{1}*/+*	17.5 ± 4.2*
Djun^{2}*/+*	16.1 ± 2.8*
Djun^{3}*/+*	13.7 ± 2.6*
Df(2R)E73 (Djun^{-}*)/+*	12.9 ± 3.9*
pnt^{D88}*/+*	24.2 ± 1.4
yan^{1}*/+*	26.4 ± 5.6
stbm^{X}*/+*	13.9 ± 1.6*
pk–sple9/+	19.3 ± 6.7
nmo^{E33}*/+*	21.2 ± 2.4
rlt^{1}*/+*	10.2 ± 2.7*
Ras1^{e2F}*/+*	28.3 ± 2.3
raf^{EA75}*/+*	26.5 ± 1.1
rl^{698}*/+*	27.8 ± 1.4
wg^{CX4}*/+*	26.2 ± 3.4
arm^{XM19}*/+*	29.1 ± 1.6
pan^{13}*/+*	27.5 ± 2.0

The percentage of ommatidia with abnormal polarity (± SD) for the genotypes heterozygous for the indicated alleles and containing one copy of the *sev–Rac*^{V12} transgene are shown. For each interaction, 300–600 ommatidia were scored in at least 3–6 independent eyes. For the control (*w*^{1118}), more than 1000 ommatidia were scored. The asterisks indicate significant suppressions ($p > 0.001$ in the Student's *t*-test).

that misoriented clusters were present from the earliest detectable stage and, thus, are primary defects (Figure 5a). These data are consistent with the analysis of loss-of-function *RhoA* mutants [6]. Strikingly, activated Rac1 affected polarity more specifically than the equivalent isoform of RhoA, arguing for specific and distinct roles of these GTPases in EPP establishment.

Nuclear RhoA signaling is necessary to transmit polarity information in the eye

Random mutagenesis of activated mammalian Rho^{V14} has led to the identification of mutations in the effector loop (a portion of the GTPase responsible for interaction with several effectors) that block either its action on cytoskeletal dynamics or on transcriptional activation of SRF [37]. The F39V mutation impedes the formation of actin stress fibers but does not interfere with the activation of SRF-mediated transcription, separating the two effects of Rho^{V14}. The mutation E40L interferes with both SRF activation and the formation of stress fibers [37].

We recapitulated the relevant mutations in the activated *Drosophila* Rho^{V14} protein (Figure 5g) and expressed them under the control of *sev–GAL4* in the eye disc (*sev>Rho*^{V14}

Figure 4

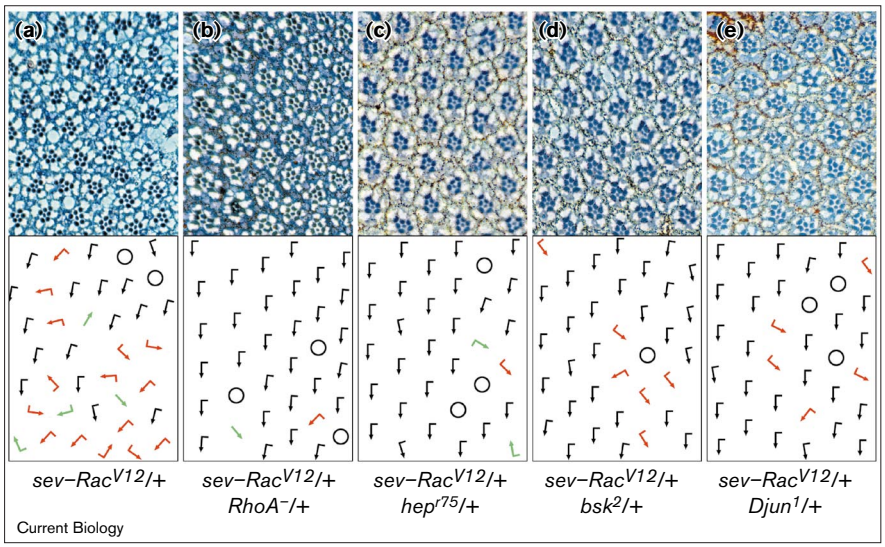

A Rac planar-polarity gain-of-function phenotype is dominantly suppressed by mutations in *RhoA* and JNK components. Tangential eye sections (upper panels) and their schematic representations (lower panels) are shown for **(a)** *sev–Rac^{V12}*/+, **(b)** *sev–Rac^{V12}*/+; *RhoA^{P2}*/+, **(c)** *sev–Rac^{V12}*/+; *hep^{r75}*/+, **(d)** *sev–Rac^{V12}*/+; *bsk^{2}*/+ and **(e)** *sev–Rac^{V12}*/+; *Djun^{1}*/+ flies. Arrows are as in Figures 1, 2 and 3. Several alleles of *bsk*, *hep* and *jun* gave similar results. Quantification of these and other interactions with *sev–Rac^{V12}* is shown in Table 1. The *sev–Rac^{V12}*/+ transgene also affected photoreceptor recruitment or differentiation. In the line shown in this figure, which was used for all the interactions, 20% of ommatidia either missed at least one photoreceptor or contained additional photoreceptors. This was increased in homozygous flies or in lines expressing the transgene at higher levels.

F39V and *sev>Rho^{V14} E40L*). The *sev>Rho^{V14} F39V* flies displayed a phenotype that was indistinguishable from that of *sev–Rho^{V14}* alone, with loss of photoreceptors and misorientation of otherwise wild-type clusters. This was evident even when the transgene was expressed at lower levels (Figure 5d). Increasing the expression levels of *sev>Rho^{V14} F39V* (two copies) led to an enhancement of both the polarity and the photoreceptor recruitment phenotypes (data not shown). In contrast, *sev>Rho^{V14} E40L* flies never displayed polarity defects, both when the transgene was expressed at low (Figure 5e) and at very high levels (Figure 5f). Nevertheless, this mutant maintained the ability of *sev>Rho^{V14}* to cause photoreceptor loss (Figure 5f): although a large number of ommatidia had lost several photoreceptors, all the remaining ommatidia with wild-type complement had the correct polarity. This indicated that removing the function required for nuclear signaling (equivalent to SRF activation in cell culture) eliminated the ability of *sev>Rho^{V14}* to induce polarity defects, suggesting that nuclear signaling by RhoA is critical for ommatidial polarity determination.

Figure 5

Nuclear signaling by RhoA affects planar-polarity generation in the eye. **(a)** Expression of β-galactosidase under the control of *svp^{07482}* in eye imaginal discs of *sev–Rho^{V14}*/*sev–Rho^{V14}* third instar larvae. Expression of β-galactosidase and its detection was as in Figure 1. The turquoise and red arrows indicate examples of correctly and abnormally oriented clusters, respectively. Part of the dorsal half of the eye disc is shown. **(b–f)** Tangential eye sections (upper panels) with corresponding schematic drawings (lower panels) from (b) *sev–Rho^{V14}*/+, (c) *sev–Rho^{V14}*/*sev–Rho^{V14}*, (d) *sev>Rho^{V14} F39V*/+, (e) *sev>Rho^{V14} E40L*/+ (weak line) and (f) *sev>Rho^{V14} E40L*/+ (strong line). The polarity versus the photoreceptor recruitment defects were quantified as the ratio between the number of ommatidia adopting an incorrect polarity and those having an abnormal complement of photoreceptors (Pol/PR). The ratios were: *sev–Rho^{V14}*/*sev–Rho^{V14}*, 0.310 ($n = 321$); *sev>Rho^{V14} F39V*/+, 0.5 ($n = 303$); *sev>Rho^{V14} E40L*/+ (weak line), 0.027 ($n = 432$) and *sev>Rho^{V14}[E40L]*/+ (strong line), 0.031 ($n = 1179$); n is the total number of ommatidia scored. **(g)** Sequence of amino acids 30–50 (in the single-letter amino-acid code) of *D. melanogaster* RhoA (DmRhoA), showing the point mutations generated in the RhoA effector loop. The residues introduced in the activated RhoA^{V14} isoform are shown in red.

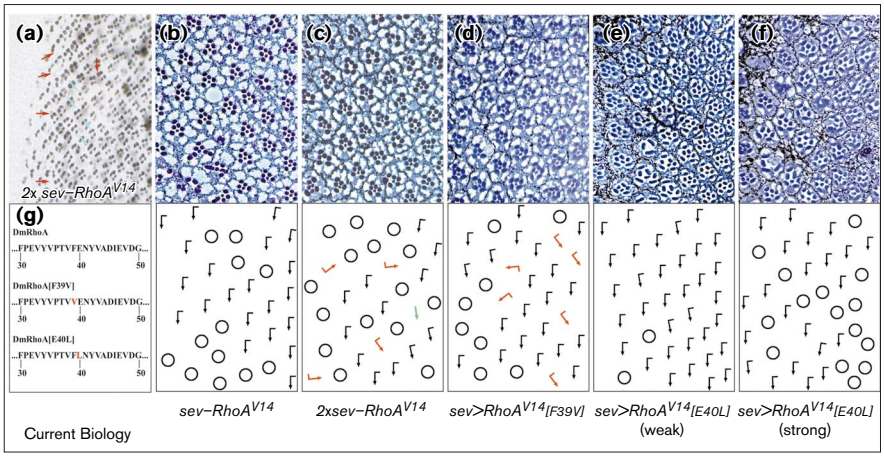

Upregulation of *puckered* and *Delta* transcription by Rac and Rho

To better characterize nuclear signaling by Rac and RhoA, we analyzed the expression of *puckered* (*puc*) and *Delta* (*Dl*). *Dl* is the only known transcriptional target of Fz signaling in R3, and *puc–lacZ* expression serves as a measure of JNK activity *in vivo*.

The *puc* gene is a transcriptional target of JNK signaling in *Drosophila*, and encodes a dual specificity protein phosphatase that acts as a negative regulator of JNK itself in a feedback loop [38,39]. In the wild type, very weak β-galactosidase expression from the *puc* enhancer trap line is detectable in all photoreceptor precursors (Figure 6a). Expression of *sev–Rac*^{V12} led to strong upregulation of *puc–lacZ* in one or, more frequently, two cells of the cluster, which could be identified as R3/R4 precursor cells, consistent with the expression pattern of *sev>Rac*^{V12} (Figure 6c). These data resemble the upregulation of *puc–lacZ* when the JNK pathway has been activated in the same cells [40].

In contrast, Rho^{V14} affected *puc–LacZ* expression differently. Although in *sev>Rho*^{V14} eye discs *puc–lacZ* expression was upregulated in some cells at a later stage (Figure 6e), these were not identifiable as the R3/R4 pair, but were often found in the position of the R2/R5/R8 precursors (where *sev* is not expressed). This suggests that the effect seen is not a direct consequence of Rho activation, but more likely a secondary effect (RhoA^{V14} E40L failed to induce significant *puc–lacZ* expression, Figure 6g). Thus, the direct transcriptional activation of *puc–LacZ* in R3/R4 correlates with the genetic interactions with the JNK module, suggesting a difference in the action of Rac and RhoA (see Discussion).

An important aspect of R3/R4 cell fate and ommatidial polarity determination is the upregulation of *Dl* expression in the R3 precursor by Fz [41,42]. Dl then signals to Notch on the R4 precursor, resulting in the choice of the R4 cell fate. In addition to Fz, other components of the Fz/planar-polarity pathway have also been found to upregulate *Dl* transcription [40]. Thus, we have investigated whether Rac and RhoA also regulate *Dl* transcription by monitoring *Dl–lacZ* expression in *sev>Rac*^{V12} and *sev>Rho*^{V14} eye discs.

In the wild type, *Dl* is expressed dynamically in photoreceptor precursors behind the furrow. Within the R3/R4 pair, it is expressed in R3 from rows 4 to 8, whereas it remains at lower levels in R4 (Figure 6b) [43]. In contrast to the difference in *puc* expression, both *sev>Rac*^{V12} and *sev>Rho*^{V14} upregulated *Dl–lacZ* expression in both R3/R4 precursors (Figure 6d,f). The RhoA^{V14} E40L isoform that is impaired in nuclear signaling did not affect *Dl* expression (Figure 6h), confirming the importance of nuclear signaling by RhoA. These effects are very similar to those of *sev–Fz* [42], supporting the idea that Rac and RhoA act downstream of Fz in the regulation of the R3/R4 cell fate. Their different effects on *puc–lacZ* indicate that their downstream effectors in nuclear signaling are distinct (see Discussion).

Figure 6

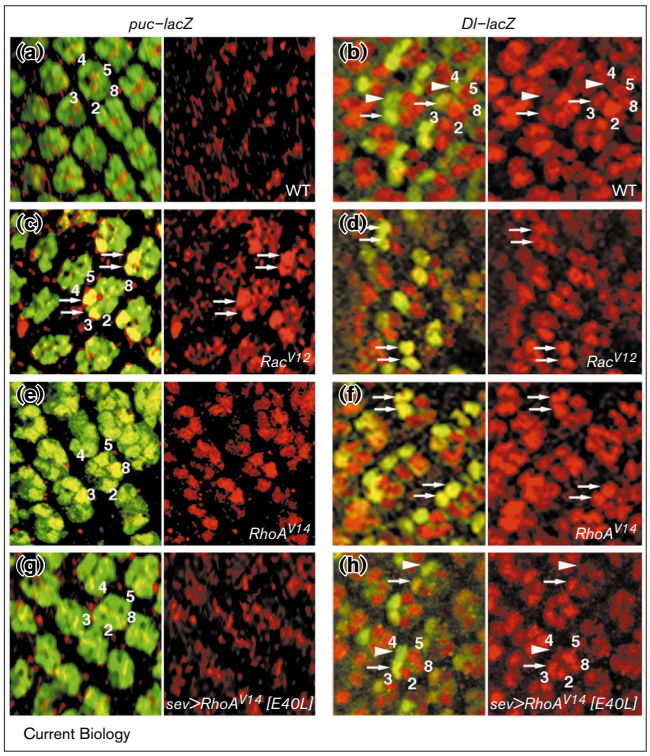

RacV12 and RhoAV14 upregulate *puc–lacZ* and *Dl–lacZ* transcription in the eye disc. Eye imaginal discs of **(a,b)** wild-type, **(c,d)** *sev>Rac*^{V12}/+, **(e,f)** *sev>Rho*^{V14}/+ and **(g,h)** *sev>Rho*^{V14} *E40L*/+ third instar larvae, heterozygous for (a,c,e,g) *puc–lacZ* or (b,d,f,h) *Dl–lacZ* are shown. Both reporter lines express a nuclear form of β-galactosidase. In each panel, the left side shows the overlay of β-galactosidase (red) and Elav (green; marks all photoreceptors); the right side shows the red channel (*puc–lacZ* or *Dl–lacZ*) only. Note that β-galactosidase was detected in both cells of the R3/R4 pair in (c) *sev>Rac*^{V12}, *puc–lacZ* and (d) *sev>Rac*^{V12}, *Dl–lacZ*. Strong upregulation appears as yellow in the overlay (left panels; examples highlighted with arrows). (e) The *sev>Rho*^{V14} transgene upregulated *puc–lacZ* (albeit to weaker levels) in R2/R5 and R8. (f) In contrast, *sev>Rho*^{V14} upregulated *Dl–lacZ* in the R3/R4 cells to the same level as did *sev>Rac*^{V12}. (g,h) No upregulation of either reporter was detected in *sev>Rho*^{V14} *E40L* discs. The precursor cells of R3/R4, R2/R5 and R8 are numbered in examples in (c–f). Examples of R3/R4 cells expressing higher levels of the reporter genes are highlighted with arrows; arrowheads mark R4 cells with lower expression.

Discussion

The finding that RhoA acts downstream of Fz [6] raised questions about the role of other members of the Rho GTPase subfamily. Are these also involved in Fz signaling, and do they act in parallel to RhoA or in a hierarchy, as has been suggested in other systems [2]? Do they exert

these effects through the cytoskeleton or is their signaling to the nucleus important for polarity establishment?

We have addressed the role of the Rac proteins in this process, using dominant-negative and activated forms of Rac1. No mutants are available in either *Rac* locus, possibly because of their high degree of similarity and potential redundancy: *Rac1* and *Rac2* are not only very similar but are also expressed in the same pattern [1–3]. It has been suggested that both could be involved in polarity signaling, as chromosomal deficiencies uncovering either *Rac1* or *Rac2* dominantly suppress *sev–Dsh* [26]. Thus, although we used Rac1 mutant isoforms, Rac2 could have a similar function and could also be affected by the expression of a dominant Rac1 mutant.

Rac is specifically required in planar-polarity signaling

We have shown that Rac is involved in Fz signaling, acting downstream of Dsh (see below). Expression of both dominant-negative Rac1 and activated Rac^{V12} mutants randomized ommatidial orientation. The similarity between the loss-of-function and gain-of-function phenotypes is a characteristic of all tissue-polarity genes, implying that the difference between the R3/R4 cells is more important than the actual level of signaling [6,26,42,44].

Using dominant-negative and activated forms of Rac, it was important to determine whether these specifically affected Rac or were generating a polarity phenotype by interfering with RhoA or other related GTPases. A specific role for Rac was supported by the enhancement of Rac^{N17} by the *Rac1* deficiency, and also by the specific interactions of the *Rac* deficiencies with *sev–Dsh* [26]. Moreover, our comparison of the *sev–*Rac^{V12} and the *sev–*Rho^{V14} phenotypes indicates that Rac and RhoA serve distinct specific roles in polarity signaling.

Role of Rac in Fz signaling

Several genetic experiments suggest that Rac acts downstream of Fz and Dsh in polarity signaling. Whereas *Rac* deficiencies dominantly suppress the *sev–Dsh* phenotype [26], taking away a copy of *fz* or *dsh* did not modify *sev–*Rac^{V12}. Moreover, *sev–*Rac^{WT} partially rescued the dsh^{1} loss-of-function allele. These data support a model in which Rac acts downstream of Fz and Dsh (Figure 7). Nevertheless, the observed phenotypes of dominant-negative Rac and Rac^{V12} are a little different from those of *fz* and *dsh*: because only few ommatidia have adopted the wrong chirality or have remained symmetrical [6,42]. A single-cell-resolution clonal analysis of *sev–*Rac^{V12}, like the one reported for *sev–Fz* [42,44], to establish whether Rac^{V12} generates the phenotype by acting within the R3/R4 pair, did not reveal a clear bias within these two cells (data not shown). Although this might suggest that the R3/R4 cell-fate decision are only partially affected by Rac, a likely alternative explanation could be the difference in expression levels of the respective transgenes. Overexpression of Rac^{V12} at higher levels causes very pleiotropic, often lethal phenotypes, impeding a more detailed analysis. However, the symmetrical clusters found in *sev–*Rac^{V12} were of the R3/R3 type and *sev>*Rac^{V12} upregulated *Dl–lacZ* in the same way as *sev–Fz*, supporting a role for Rac in R3 specification and chirality determination.

Figure 7

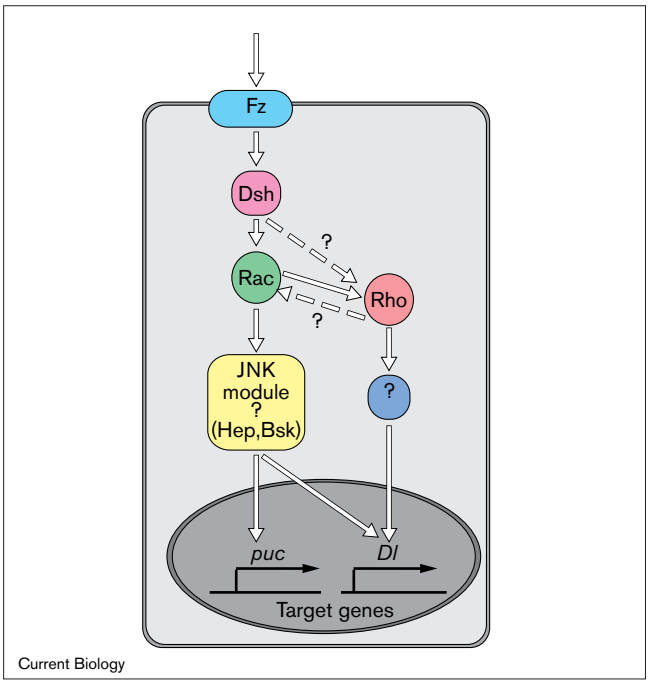

A model showing where Rac acts in the planar-polarity pathway during eye development. See text for details. The question marks indicate uncertainties of information flow and unknown components of the pathway.

We have observed that dominant-negative Rac, which impairs the Fz signaling pathway, is also able—when enhanced by *Df(3L)emc5* or *RhoA* mutants—to generate R3/R3 symmetrical ommatidia (in addition to the R4/R4 type) and is phenotypically similar to fz^{-} and dsh^{-} mutant backgrounds, where both R3/R3 and R4/R4 symmetrical ommatidia are found [6,16,27]. This suggests that, in the absence of Fz signaling, the generation of ommatidial chirality and R3/R4 specification relies on a stochastic activation (or inactivation) of Notch [41,42,44]. In contrast, hyperactivation of Fz signaling (for example, in *sev–Fz*), consistently pushes both cells to the R3 fate, generating predominantly R3/R3 symmetrical ommatidia [42,44].

Relationship between Rac and Rho and importance of their signaling to the nucleus

How do Rac and Rho relate to each other? *RhoA* mutations suppressed *sev–*Rac^{V12} and enhanced *sev>*Rac^{N17}. In

addition, the expression of wild-type RhoA (partially) rescued the *sev>Rac^{N17}* phenotype. These data support two models. Firstly, RhoA could be acting downstream of Rac (Figure 7). Alternatively, RhoA could be activated independently of Rac by upstream molecules (like Dsh) but then, acting in parallel, would influence (and be influenced by) Rac. We favor the first scenario because of the absence of genetic interactions between the Rac deficiencies and activated RhoA.

We determined whether their effects were due to their action on the cytoskeleton. An indication that Rac signaling to the nucleus is important were its specific genetic interactions with the JNK pathway components *hep*, *bsk* and *jun*. This is consistent with cell culture experiments, in which Rac activates JNK, and with the observation that JNK components suppress *sev–Fz* and *sev–Dsh* [6,26,32]. Nevertheless, the role of JNK signaling in the establishment of ommatidial polarity is still unclear, as analysis of loss-of-function alleles of *hep* and *bsk* has not detected polarity defects [26,32,40].

To gain an insight into the importance of nuclear signaling by RhoA, we introduced specific mutations in its effector loop, which separate its action on the cytoskeleton from the ability to signal to the nucleus [37]. Strikingly, *sev>Rho^{V14} F39V* was indistinguishable from *sev–Rho^{V14}* in its effects on polarity, whereas *sev>Rho^{V14} E40L* was significantly different (not affecting planar polarity), implying that nuclear signaling is important in this context.

To investigate the role of Rac and RhoA further, we determined whether their activated forms could upregulate the expression of *puc*, a transcriptional target of JNK, and *Dl*, the only known Fz target. Both GTPases, like *sev–Fz*, caused an upregulation of *Dl*, supporting the idea that Fz-mediated nuclear signaling is relayed by these GTPases. In contrast, monitoring the level of expression of *puc* in the eye disc revealed a difference between Rac and RhoA. Whereas upregulation of *puc* by *sev–Rac^{V12}* in R3/R4 is consistent with the genetic interactions, the weaker *puc* activation by *sev–Rho^{V14}* in R2/R5 and R8 suggests that this is a secondary effect. This difference suggests that nuclear signaling by Rac and RhoA is mediated by distinct downstream effectors, possibly JNK for Rac and yet unknown components for RhoA (Figure 7).

Nevertheless, these observations do not rule out the possibility that the same GTPases are also required to modify the cytoskeleton of the photoreceptor precursors. It is likely that a dynamic developmental system, requiring cells to move and rotate in a co-ordinated fashion, is achieved through modifications of the cytoskeleton, which can be induced by these small GTPases at the same time as Fz-induced nuclear signaling (as well as at later stages).

The presence of multiple Rac proteins, and their closely related Rho family members RhoA and Cdc42, in *Drosophila* makes an analysis of the specific requirements of each single GTPase difficult in loss-of-function studies. Moreover, their pleiotropic requirements in many processes further hampers a detailed analysis in specific contexts. Thus, the approach used here provides an insight into their roles in the context of Dsh-mediated planar-polarity signaling. Further experiments will be necessary to refine their detailed roles and identify their specific effectors in this context.

Conclusions

We have provided evidence that Rac acts downstream of Dsh in the Fz-mediated planar-polarity pathway (Figure 7). Rac appears to function upstream or in parallel to RhoA in this process. Both Rac and RhoA signal to the nucleus, possibly through distinct effectors, to regulate *Dl* expression in R3 and planar-polarity determination in the *Drosophila* eye.

Supplementary material

Supplementary material including full methodological details is available at http://current-biology.com/supmat/supmatin.htm.

Acknowledgements

We are grateful to L. Luo, R. Barrio, M. Fortini, K. Basler and G. Rubin for fly strains and reagents. We thank A.-M. Voie for embryo injections; R. Wepf and A. Cyrklaff for help with scanning electron microscopy analysis and chromosome *in situ* mapping, respectively; S. Eaton and N. Paricio for helpful discussions; and J. Curtiss for helpful comments on the manuscript. D.I.S. was a recipient of an EEC postdoctoral fellowship.

References

1. Luo L, Liao YJ, Jan LY, Jan YN: **Distinct morphogenetic functions of similar small GTPases: *Drosophila* Drac1 is involved in axonal outgrowth and myoblast fusion.** *Genes Dev* 1994, **8:**1787-1802.
2. Harden N, Loh HY, Chia W, Lim L: **A dominant inhibitory version of the small GTP-binding protein Rac disrupts cytoskeletal structures and inhibits developmental cell shape changes in *Drosophila*.** *Development* 1995, **121:**903-914.
3. Hariharan IK, Hu K-Q, Asha H, Quintanilla A, Ezzell RM, Settleman J: **Characterisation of Rho GTPase family homologues in *Drosophila melanogaster*: overexpressing *Rho1* in retinal cells causes a late developmental defect.** *EMBO J* 1995, **14:**292-302.
4. Glise B, Noselli S: **Coupling of Jun amino-terminal kinase and Decapentaplegic signaling pathways in *Drosophila* morphogenesis.** *Genes Dev* 1997, **11:**1738-1747.
5. Eaton S, Auvinen P, Luo L, Jan YN, Simons K: **CDC42 and Rac1 control different actin-dependent processes in the *Drosophila* wing disc epithelium.** *J Cell Biol* 1995, **131:**151-164.
6. Strutt DI, Weber U, Mlodzik M: **The role of RhoA in tissue polarity and Frizzled signalling.** *Nature* 1997, **387:**292-295.
7. Blair S: **Eye development: Notch lends a handedness.** *Curr Biol* 1999, **9:**356-360.
8. Reifegerste R, Moses K: **The genetics of epithelial polarity and pattern in the *Drosophila* retina.** *Bioessays* 1999, **21:**275-285.
9. Mlodzik M: **Planar polarity in the *Drosophila* eye: a multifaceted view of signaling specificity and cross-talk.** *EMBO J* 1999, **24:**6873-6879.
10. Ready DF, Hanson TE, Benzer S: **Development of the *Drosophila* retina, a neurocrystalline lattice.** *Dev Biol* 1976, **53:**217-240.
11. Tomlinson A: **Cellular interactions in the developing *Drosophila* eye.** *Development* 1988, **104:**183-193.
12. Wolff T, Ready DF: **The beginning of pattern formation in the *Drosophila* compound eye: the morphogenetic furrow and the second mitotic wave.** *Development* 1991, **113:**841-850.
13. Adler PN: **The genetic control of tissue polarity in *Drosophila*.** *Bioessays* 1992, **14:**735-741.

14. Gubb D, García-Bellido A: **A genetic analysis of the determination of cuticular polarity during development in *Drosophila melanogaster*.** *J Embryol Exp Morphol* 1982, **68:**37-57.
15. Theisen H, Purcell J, Bennett M, Kansagara D, Syed A, Marsh JL: ***dishevelled* is required during *wingless* signalling to establish both cell polarity and cell identity.** *Development* 1994, **120:**347-360.
16. Zheng L, Zhang J, Carthew RW: ***frizzled* regulates mirror-symmetric pattern formation in the *Drosophila* eye.** *Development* 1995, **121:**3045-3055.
17. Vinson CR, Adler PN: **Directional non-cell autonomy and the transmission of polarity information by the *frizzled* gene of *Drosophila*.** *Nature* 1987, **329:**549-551.
18. Vinson CR, Conover S, Adler PN: **A *Drosophila* tissue polarity locus encodes a protein containing seven potential transmembrane domains.** *Nature* 1989, **338:**263-264.
19. Bhanot P, Brink M, Samos CH, Hsieh J-C, Wang Y, Macke JP, Andrew D, *et al.*: **A new member of the *frizzled* family from *Drosophila* functions as a Wingless receptor.** *Nature* 1996, **382:**225-230.
20. Cadigan KM, Fish MP, Rulifson EJ, Nusse R: **Wingless repression of *Drosophila* frizzled2 expression shapes the Wingless morphogen gradient in the wing.** *Cell* 1998, **93:**767-777.
21. Bhat KM: **Frizzled and Frizzled2 play a partially redundant role in Wingless signaling and have similar requirements to Wingless in neurogenesis.** *Cell* 1998, **95:**1027-1036.
22. Kennerdell JR, Carthew RW: **Use of dsRNA-mediated genetic interference to demonstrate that *frizzled* and *frizzled2* act in the *wingless* pathway.** *Cell* 1998, **95:**1017-1026.
23. Mueller H, Samanta R, Wieschaus E: **Wingless signaling in the *Drosophila* embryo: zygotic requirements and the role of the *frizzled* genes.** *Development* 1999, **126:**577-586.
24. Bhanot P, Fish M, Jemison JA, Nusse R, Nathans J, Cadigan KM: **Frizzled and DFrizzled-2 function as redundant receptors for wingless during *Drosophila* embryonic development.** *Development* 1999, **126:**4175-4186.
25. Axelrod JD, Miller JR, Shulman JM, Moon RT, Perrimon N: **Differential requirement of Dishevelled provides signaling specificity in the Wingless and planar cell polarity signaling pathways.** *Genes Dev* 1998, **12:**2610-2622.
26. Boutros M, Paricio N, Strutt DI, Mlodzik M: **Dishevelled activates JNK and discriminates between JNK pathways in planar polarity and *wingless* signaling.** *Cell* 1998, **94:**109-118.
27. Krasnow RE, Wong LL, Adler PN: ***dishevelled* is a component of the *frizzled* signalling pathway in *Drosophila*.** *Development* 1995, **121:**4095-4102.
28. Choi K-W, Benzer S: **Rotation of photoreceptor clusters in the developing *Drosophila* eye requires the *nemo* gene.** *Cell* 1994, **78:**125-136.
29. Eaton S, Wepf R, Simons K: **Roles for Rac1 and Cdc42 in planar polarization and hair outgrowth in the wing of *Drosophila*.** *J Cell Biol* 1996, **135:**1277-1289.
30. Mlodzik M, Hiromi Y, Weber U, Goodman CS, Rubin GM: **The *Drosophila seven-up* gene, a member of the steroid receptor gene superfamily, controls photoreceptor cell fates.** *Cell* 1990, **60:**211-224.
31. Fanto M, Mayes CA, Mlodzik M: **Linking cell-fate specification to planar polarity: determination of the R3/R4 photoreceptors is a prerequisite for the interpretation of the Frizzled mediated polarity signal.** *Mech Dev* 1998, **74:**51-58.
32. Paricio N, Feiguin F, Boutros M, Eaton S, Mlodzik M: **The *Drosophila* STE20-like kinase Misshapen is required downstream of the Frizzled receptor in planar polarity signaling.** *EMBO J* 1999, **18:**4669-4678.
33. Minden A, Lin A, Claret F-X, Abo A, Karin M: **Selective activation of the JNK signaling cascade and c-Jun transcriptional activity by the small GTPases Rac and Cdc42Hs.** *Cell* 1995, **81:**1147-1157.
34. Coso OA, Chiariello M, Yu J-C, Teramoto H, Crespo P, Xu N, Miki T, Gutkind JS: **The small GTP-binding proteins Rac1 and Cdc42 regulate the activity of the JNK/SAPK signaling pathway.** *Cell* 1995, **81:**1137-1146.
35. Wolff T, Rubin GM: ***strabismus*, a novel gene that regulates tissue polarity and cell fate decisions in *Drosophila*.** *Development* 1998, **125:**1149-1159.
36. Gubb D, Green C, Huen D, Coulson D, Johnson G, Tree D, Collier S, Roote J: **The balance between isoforms of the prickle LIM domain protein is critical for planar polarity in *Drosophila* imaginal discs.** *Genes Dev* 1999, **13:**2315-2327.
37. Sahai E, Alberts AS, Treisman R: **RhoA effector mutants reveal distinct effector pathways for cytoskeletal reorganization, SRF activation and transformation.** *EMBO J* 1998, **17:**1350-1361.
38. Glise B, Bourbon H, Noselli S: **Hemipterous encodes a novel MAP kinase kinase required for epithelial cell sheet movement.** *Cell* 1995, **83:**451-461.
39. Martin-Blanco E, Gampel A, Ring J, Virdee K, Kirov N, Tolkowsky AM, Martinez-Arias A: ***puckered* encodes a phosphatase that mediates a feedback loop regulating JNK activity during dorsal closure in *Drosophila*.** *Genes Dev* 1998, **12:**557-570.
40. Weber V, Pariscio N, Mlodzik M: **Jun mediates Frizzled-induced R3/R4 cell fate distinction and planar polarity determination in the *Drosophila* eye.** *Development* 2000, **127:**3619-3629.
41. Cooper MTD, Bray SJ: **Frizzled regulation of Notch signalling polarizes cell fate in the *Drosophila* eye.** *Nature* 1999, **397:**526-529.
42. Fanto M, Mlodzik M: **Asymmetric Notch activation specifies photoreceptors R3 and R4 and planar polarity in the *Drosophila* eye.** *Nature* 1999, **397:**523-526.
43. Parks AL, Turner FR, Muskavitch MAT: **Relationships between complex Delta expression and the specification of retinal cell fates during *Drosophila* eye development.** *Mech Dev* 1995, **50:**201-216.
44. Tomlinson A, Struhl G: **Decoding vectorial information from a gradient: sequential roles of the receptors Frizzled and Notch in establishing planar polarity in the *Drosophila* eye.** *Development* 1999, **126:**5725-5738.

Because *Current Biology* operates a 'Continuous Publication System' for Research Papers, this paper has been published on the internet before being printed. The paper can be accessed from http://biomednet.com/cbiology/cub – for further information, see the explanation on the contents page.

Supplementary material

Nuclear signaling by Rac and Rho GTPases is required in the establishment of epithelial planar polarity in the *Drosophila* eye

Manolis Fanto, Ursula Weber, David I. Strutt and Marek Mlodzik

Current Biology 1 August 2000, **10**:979–988

Supplementary materials and methods

Histology and immunofluorescence

Antibody staining of eye imaginal discs and sections of adult retinae were performed as described [S1]. Antibodies used were: rabbit anti-β-galactosidase (Sigma, 1/2000 dilution), rat monoclonal anti-Elav (1/50 dilution), and rat anti-Spalt (kindly provided by R. Barrio, at 1/50). Secondary antibodies conjugated with FITC or RITC were from Jackson Labs. Secondary antibodies conjugated with horseradish peroxidase (HRP) were from Biorad. Following antibody stainings, eye imaginal discs were mounted in Mowiol and viewed with Zeiss Axiophot or Leica confocal microscopes. For scanning electron microscopy, heads were prepared by critical point drying and coated with 2 nm gold.

Fly strains and genetic interactions

The *UAS–Rac^{N17}* and the *UAS–Rac^{V12}* flies were kindly provided by L. Luo [S2]. The *sev>Rac^{N17}* and *sev>Rac^{V12}* strains are recombinants with a *sev–Gal4* driver (gift of K. Basler). The *sev–Rac^{V12}* and *sev–Rac* strains were generated by cloning the respective cDNAs into the pSevE vector, which carries three copies of the *sev* enhancer and the *sev* promoter (provided by M.Fortini) [S3]. Germ-line transformation was performed by standard procedures [S4].

Constructs for expression of Rho^{V14}, Rho^{V14} F39V and Rho^{V14} E40L were generated by PCR-mediated *in vitro* mutagenesis and cloned into the pUAST vector [S5] to generate *UAS–Rho^{V14}, UAS–Rho^{V14} F39V* and UAS–*Rho^{V14} E40L* fly stocks. *UAS–Rho^{wt}* served as control stock; *sev>Rho^{V14}, sev>Rho^{V14} F39V* and *sev>Rho^{V14} E40L* are recombinants with *sev–GAL4*, as is *sev>Rac^{N17}*. All genetic interactions were carried out at 25°C, except in the case of the interactions with *sev>Rac^{N17}*, which were performed at 18°C.

The following mutant lines, described in Flybase, were used: *fz^{1}, dsh^{V26}, dsh^{1}, RhoA^{P2}, RhoA^{72R}, Cdc42^{3}, Df(3L)emc5, hep^{1}, hep^{r75}, bsk^{1}, bsk^{2}, Djun^{1}, Djun^{2}, Djun^{3}, Df(2R)E73, pnt^{D88}, yan^{1}, pk-sple^{9}, nmo^{E33}, rlt^{1}, Ras1^{e2F}, raf^{EA75}, rl^{698}, wg^{CX4}, arm^{XM19},* and *pan^{13}*. The *stbm^{X}* allele was identified as a spontaneous mutation in our lab (N. Paricio, unpublished data). The *svp* enhancer detector line, *svp^{07482}*, the *puc–lacZ* and *Dl–lacZ* reporter lines were as described [S6,S7,S8].

Supplementary references

S1. Tomlinson A, Ready DF: **Neuronal differentiation in the *Drosophila* ommatidium.** *Dev Biol* 1987, **120:**366-376.

S2. Luo L, Liao YJ, Jan LY, Jan YN: **Distinct morphogenetic functions of similar small GTPases: *Drosophila* Drac1 is involved in axonal outgrowth and myoblast fusion.** *Genes Dev* 1994, **8:**1787-1802.

S3. Fortini ME, Simon MA, Rubin GM: **Signalling by the *sevenless* protein tyrosine kinase is mimicked by Ras1 activation.** *Nature* 1992, **355:**559-561.

S4. Spradling AC, Rubin GM: **Transposition of cloned *P* elements into *Drosophila* germ line chromosomes.** *Science* 1982, **218:**341-347.

S5. Brand AH, Perrimon N: **Targeted gene expression as a means of altering cell fates and generating dominant phenotypes.** *Development* 1993, **118:**401-415.

S6. Fanto M, Mayes CA, Mlodzik M: **Linking cell-fate specification to planar polarity: determinationof the R3/R4 photoreceptors is a prerequisite for the interpretation of the Frizzled mediated polarity signal.** *Mech Dev* 1998, **74:**51-58.

S7. Martin-Blanco E, Gampel A, Ring J, Virdee K, Kirov N, Tolkowsky AM, Martinez-Arias A: ***puckered* encodes a phosphatase that mediates a feedback loop regulating JNK activity during dorsal closure in *Drosophila*.** *Genes Dev* 1998, **12:**557-570.

S8. Fanto M, Mlodzik M: **Asymmetric Notch activation specifies photoreceptors R3 and R4 and planar polarity in the *Drosophila* eye.** *Nature* 1999, **397:**523-526.